BMC Musculoskeletal Disorders

RESEARCH

Open Access

Role of IL-16 in age-related skeletal muscle atrophy: an integrated study

Wenliang Fan[1], Zhibang Zhao[1], Liqiang Wang[1] and Qingbo Chu[1*]

Abstract

Background In this study, we aim to explore the roles of IL-16 in sarcopenia based on older orthopedic patients and animal research.

Methods This clinical research in this study was an observational investigation and included all the older patients with orthopedic trauma admitted to our department between January 2021 and January 2022. Patients were identified with sarcopenia if they have both low hand grip strength (HGS) and low appendicular skeletal muscle mass (ASM). Propensity score matching (PSM) was performed to reduce the bias caused by the co-factors and levels of IL-16 between normal patients and patients with sarcopenia were compared. In animal research, mice were treated with IL-16 to identify the effects of IL-16 on muscle function and muscle mass. Then the sarcopenia models were established and the anti-IL-16 was performed to identify the potential therapeutical effect of targeting IL-16.

Results 421 individuals were included in the clinical study, and 77 were identified as sarcopenia. In the matched populations, the serum levels of IL-16 of individuals with low HGS, ASM, and sarcopenia were significantly higher than normal individuals (all $p < 0.001$). The mice treated with IL-16 showed significantly impaired muscle function and physical performance and loss of muscle mass. Using anti-IL-16 antibodies may rescue the sarcopenia traits caused by botulinum toxin type A.

Conclusion Individuals with high levels of IL-16 may have a significantly high risk of sarcopenia. IL-16 impairs muscle function and physical performance and leads to muscle atrophy in mice, and these effects could be reduced by targeting IL-16.

Keywords IL-16, Sarcopenia, Inflammaging, Cytokines, Muscle atrophy

Introduction

Sarcopenia refers to the progressive loss of skeletal muscle mass and function that occurs with aging, characterized by a decrease in muscle strength, power, and physical performance, which can lead to reduced mobility and an increased risk of falls and fractures [1]. Sarcopenia is associated with a decline in muscle fiber size and number, particularly type II muscle fibers, and an increase in fat infiltration within the muscle tissue [2].

Though the understanding of the etiology of sarcopenia is still limited, studies have proven that the etiology of sarcopenia is multifactorial, involving both intrinsic aging processes and extrinsic factors [3]. Previous studies have reported the roles of age, immune status, lifestyle, nutrition, and chronic diseases in the development of sarcopenia. In all these factors, advanced age is a significant risk factor for sarcopenia [4].

*Correspondence:
Qingbo Chu
13721809268@163.com
[1]Emergency Trauma Center, Nanyang Second People's Hospital, No 66, East Jianshe Road, Nanyang 473000, Henan, China

In recent years, inflammaging, the chronic low-grade inflammation that occurs with aging, has attracted increasing interest from researchers around the world [5]. Inflammaging is associated with an increase in the systemic levels of pro-inflammatory molecules, such as tumor necrosis factor-alpha (TNF-α), interleukin-6 (IL-6), interleukin-1 (IL-1), and chemokines [6]. These inflammatory molecules may contribute to tissue degeneration and the pathogenesis of age-related diseases, including sarcopenia [7].

Understanding the roles of inflammaging in sarcopenia is crucial for developing strategies to prevent and manage sarcopenia and provide novel insights for immune aging. Interleukin-16 (IL-16) is a pro-inflammatory cytokine that plays a significant role in immune regulation and inflammation, which may contribute to chronic inflammation in older individuals [8]. Originally identified as a lymphocyte chemoattractant factor, IL-16 is chemotactic for CD4 + T lymphocytes, monocytes, and eosinophils, and it can upregulate IL-2 receptor and HLA-DR expression, inhibit T cell receptor (TcR)/CD3-dependent activation, and promote repression of HIV-1 transcription [9].

Previous studies have reported the potential role of IL-16 in sarcopenia, but most of them were based on estimation, with limited sample size and lack of strong evidence [10]. In this study, we aim to comprehensively explore the relationship between serum levels of IL-16 and sarcopenia. We hypothesized that IL-16 may lead to muscle atrophy and a decline in muscle function. By integrating the evidence from the population of older adults and experiments based on mice, we try to identify the correlation between serum levels of IL-16 and sarcopenia and explore the impact of IL-16 in the development of sarcopenia in mice. Specifically, the botulinum toxin type A (BoNT/A) model, a widely used sarcopenia model in preclinical studies [11], was established and treated by anti-IL-16 antibodies, which may potentially suggest the therapeutical effect of targeting IL-16. By understanding the roles of IL-16 in sarcopenia, we may develop advanced strategies targeting IL-16 to prevent and manage sarcopenia, ultimately improving the quality of life and health outcomes in older adults.

Methods

Study population

This clinical research in this study was an observational investigation conducted at the Emergency Trauma Center of Nanyang Second People's Hospital, Nanyang, Henan Province, China. The study was conducted in accordance with the tenets delineated in the Declaration of Helsinki and obtained approval from the Ethics Committee of Nanyang Second People's Hospital (ID: 2020 Research Review No. 11). We included all the older patients with orthopedic trauma admitted to our department between January 2021 and January 2022. The inclusion criteria were: (a) age ≥ 60 years; (b) injury severity score (ISS) ≤ 8; (c) with informed consent; The exclusion criteria were: (a) pathological fractures; (b) with immune-related diseases that prevent accurate IL-16 measurements; (c) with diseases or fractures that prevent accurate sarcopenia measurements. The patients who met the inclusion and exclusion criteria were finally enrolled in this study (Fig. 1). Stringent measures were implemented to safeguard patient confidentiality and explicit written consent was procured from all enrolled individuals.

Clinical data

The baseline data of the participants were collected from electronic medical records of our hospital, including age, sex, body mass index (BMI), fracture history, smoking and alcohol use history, comorbidities, electrocardiogram evaluations, and chest X-ray evaluations. The Charlson comorbidity index (CCI) was used to quantify the presence and impact of these comorbid conditions. The measurement of serum IL-16, red blood cell count (RBC), hemoglobin levels (Hb), blood glucose levels (GLU), and albumin levels (ALB) were conducted in the department of laboratory when the patient was first admitted. The normal laboratory measurements were conducted by using the hospital's routine laboratory equipment (Sysmex XE-2100, Kehua Bio-engineering Co., Ltd., Shanghai, China; TBA-120FR, Toshiba Co., Ltd., Tokyo, Japan), and the data were collected from the electronic medical record. Serum IL-16 was measured by using a human IL-16 ELISA kit (JL19254-96T, Jonlnbio).

Measurement of sarcopenia

In our study, the diagnosis of sarcopenia was conducted following the criteria established by the Asian Working Group for Sarcopenia (AWGS) [1]. Patients were identified with sarcopenia if they have both low hand grip strength (HGS) and low appendicular skeletal muscle mass (ASM). Specifically, HGS was considered low if it was below 28 kg for males and below 18 kg for females. ASM was deemed low if it was less than 7.00 kg/m^3 for males and less than 5.70 kg/m^3 for females.

HGS was assessed using a spring-loaded dynamometer. Given the compromised mobility of participants with hip fractures, HGS measurements were performed in a seated position. Each participant's HGS was measured three times, and the maximum value was recorded for analysis. For the quantification ASM, bioimpedance analysis (BIA) was employed, utilizing the InBody BWA2.0 device (InBody Co. Ltd., Shanghai, China). This methodology involved the application of forty bioimpedance measurements across a range of eight distinct frequencies (1 kHz, 5 kHz, 50 kHz, 250 kHz, 500 kHz, 1 MHz,

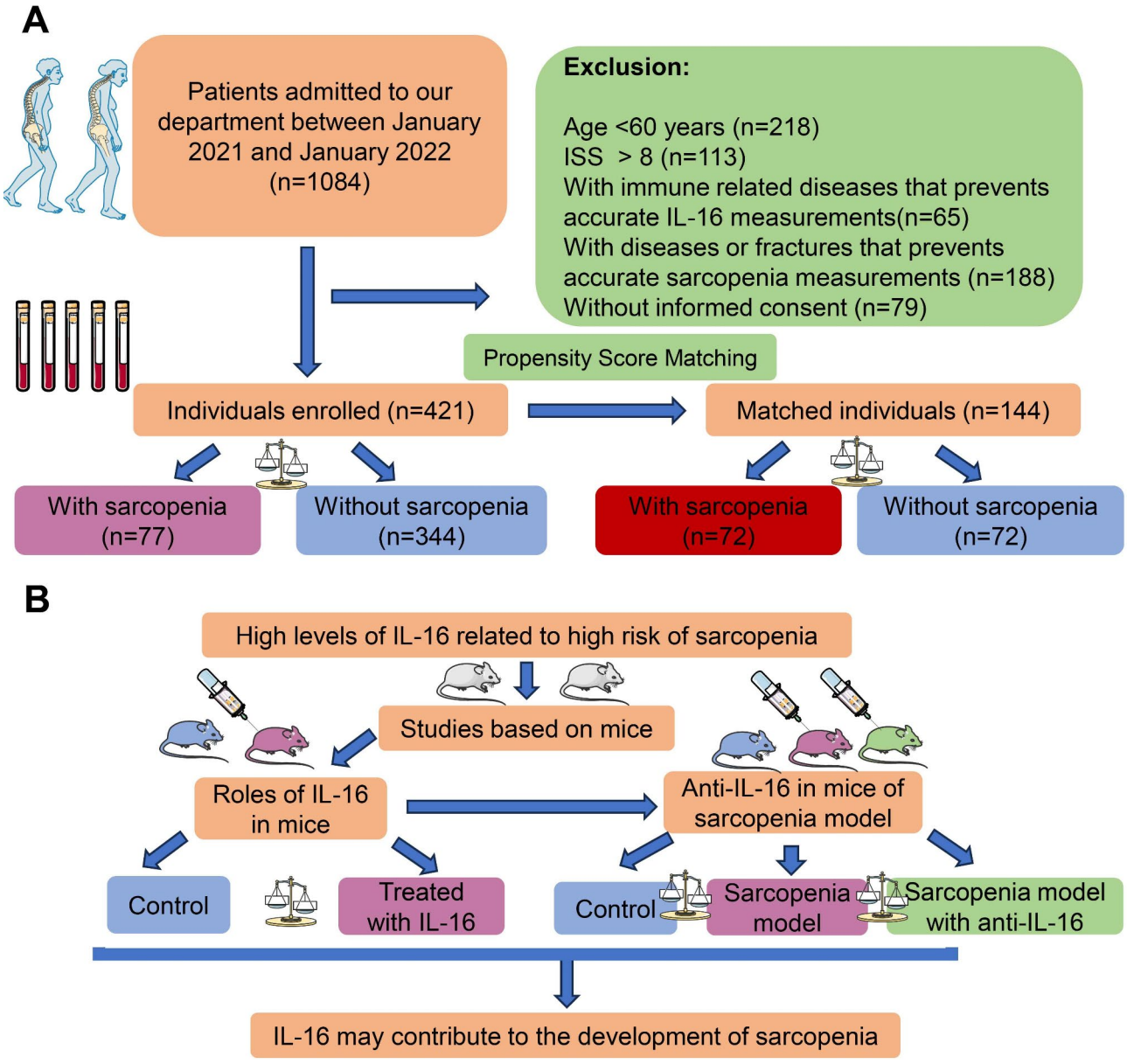

Fig. 1 Flow chart of our study. **A**: Study design of population study; **B**: Study design of animal study

2 MHz, 3 MHz) to five segmental regions of the body: right upper limb, left upper limb, trunk, right lower limb, and left lower limb. The device's integrated calculation model amalgamated these measurements to automatically determine ASM, which was subsequently normalized for height to account for variations in stature among participants.

Animals

The animal studies were reviewed and approved by the Animal Ethics Committee of Nanyang Second People's Hospital (ID: 2021 Animal Research Review No. 2), and C57BL/6 N mice were purchased from Zhengzhou Antu Biological Engineering Co., LTD. All mice were housed in a controlled environment with a stable temperature ranging from 68 °F to 76 °F, relative humidity levels between 30% and 70%, within a pathogen-free area, and experienced a consistent 12-hour cycle of light and darkness. Prior to euthanasia, animals were rendered fully unconscious via intraperitoneal injection of sodium pentobarbital (60 mg/kg body weight). Following confirmation of deep anesthesia, cervical dislocation was applied to ensure death. Death was verified by absence of spontaneous breathing, pupil dilation, and palpable heartbeat for ≥ 5 min.

Models and treatments

All animals were raised to an age of 14 months to emulate the characteristics of aging, after which the experiments were initiated. For the sarcopenia model [11], mice were administered an intramuscular injection of 1 unit (U) of Botulinum Toxin Type A (BoNT/A, 20200862; Hengli), evenly distributed into both limbs, with a total injection volume of 20 μL of physiological saline, administered biweekly. In the IL-16 blocking group, mice received intraperitoneal injections of either mouse IgG (400264, BioLegend) or anti-IL-16 (519108, BioLegend) antibody at a dosage of 10 mg/kg, administered every three days [12]. For the IL-16 supplementation group, mice were intraperitoneally injected with recombinant mouse IL-16 protein (90152ES76; Yeasen) at a dosage of 50 μg/kg, administered every three days.

ELISA

The serum IL-16 levels of mice were measured using the IL-16 mouse ELISA kit (JL20249-96T, Jonlnbio) according to the protocols of the kits. Briefly, serum samples from mice were collected and processed according to the kit's instructions, ensuring that they were free from contaminants that could interfere with the assay. Samples were added to antibody-coated plates, and after incubation and washing, bound IL-16 was detected using HRP-conjugated antibodies and a colorimetric substrate. The absorbance was measured, and IL-16 concentrations were determined from a standard curve constructed with known concentrations of IL-16. Using similar experimental protocols, we also measured serum IL-6 (JL20268-96T, Jonlnbio) and TNFA (JL10484-96T, Jonlnbio) concentrations.

Quantitative real-time polymerase chain reaction (qRT-PCR)

Total RNA was extracted from skeletal muscle samples using TRIzol reagent (Ambion, Thermo Fisher, Germany). The concentration and purity of the RNA were quantified using a NanoVue spectrophotometer (GE Healthcare, Germany). Subsequently, cDNA was synthesized from the RNA samples using the PrimeScript™ RT reagent kit (Takara, Otsu, Shiga, Japan) according to the manufacturer's instructions. Quantitative real-time PCR (qRT-PCR) was performed on a 7900HT Fast Real-Time PCR System (Applied Biosystems, Foster City, CA, USA) with TB Green Premix Ex Taq™ II (Takara, Otsu, Shiga, Japan). The relative mRNA expression levels were calculated using the $2 - \Delta\Delta CT$ method and normalized to GAPDH expression. The sequences of the PCR primers used in this study are as follows: GAPDH (Forward, CC ATTCTTCCACCTTTGATGCT-3; Reverse, GTTGCTG TAGCCATATTCATTGT), MHC-I (Forward, AGATGA ATGCCGAGCTCACT; Reverse, CTCATCCAAACCAG CCATCT); MHC-IIa (Forward, GAGCAA AGATGCAG GGAAAG; Reverse, TAAGGGTTGACGGTGACACA); MHC-IIb: (Forward, GGGGCTGTACCAGAAATCCG; Reverse, CCTGAAGAGAGCTGACA CGG); MHC-IIx (Forward, AGAAGCTCCTGGGATCCATT; Reverse, CT CTCGCCAAGTACCCTCTG).

Physical performance evaluation

Animals were subjected to a 10° inclined treadmill (SansBio) with an initial speed set at 6 cm/s, which was incremented by 1 cm/s every 1 min. Exhaustion was determined when a mouse's hindlimbs remained in contact with the electric grid for over 15 s, and the measurement of time paused during the period when a mouse made electric grid contact. The distance and time to exhaustion were calculated according to the treadmill data. 24 h after the test of exhaustion, mice were exposed to a treadmill exercise regimen at varying speeds—6, 8, 10, 12, 14, and 16 m/min—for 3-minute intervals to assess their recovery capacity following muscle exhaustion.

Ectopic lipid content

Total lipids were extracted from the quadriceps using the Folch method, as previously described [13]. Briefly, tissue samples were homogenized in a 2:1 chloroform-methanol mixture to facilitate lipid extraction. The homogenate was incubated at 4 °C for 1 h to allow for optimal lipid solubilization. Following incubation, the mixture was centrifuged at 2400× g for 10 min to separate the phases. Subsequently, 0.2 volumes of 0.88% sodium chloride were added to the homogenate to further aid phase separation. After centrifugation, the lower phase containing the lipid fraction was collected, washed, and dried under ambient conditions to obtain the lipid extract.

Histological analysis and Immunofluorescence staining

Skeletal muscle samples were embedded in an optimal cutting temperature compound and rapidly frozen in isopentane pre-chilled with liquid nitrogen, followed by storage at -80 °C until further use. Cryosections were generated using a Leica CM3054 cryostat. Hematoxylin and eosin (H&E) staining was performed on 10-micrometer-thick transverse sections taken at the mid-belly of the muscle. The cross-sectional area (CSA) of muscle fibers was evaluated using a high-magnification field on a Nikon Eclipse TS100 optical microscope, which was coupled with a Nikon D5100 digital camera for image acquisition. The quantitative analysis was performed using ImageJ software version 1.53.

For immunofluorescence staining, 10-micrometer-thick frozen tissue sections were fixed with a 4% paraformaldehyde solution for 10 min at ambient temperature. Following PBS rinsing, slides were blocked with a 5%

bovine serum albumin (BSA) in PBS solution for 1 h. The slides were then incubated with primary antibodies (Rabbit polyclonal to Laminin, ab11575, abcam) at 4 °C for an extended period. After thorough PBS washing, the slides were incubated with the corresponding secondary antibodies diluted at 1:400 (Goat Anti-Rabbit IgG H&L Alexa Fluor® 488, ab150077, abcam) for 1 h at room temperature. Images were obtained using a Zeiss Axio Imager 2, and the quantitative analysis was performed using ImageJ software version 1.53.

Statistical analyses

Continuous variables were reported as mean ± standard deviation and categorical variables were expressed as counts with percentages. For two-group comparisons, independent student's t-tests were used for data exhibiting normal distribution, and Wilcoxon rank-sum tests were used for non-normally distributed data. For multiple group comparisons, ANOVA with Turkey's post-tests was conducted. Categorical variables were evaluated with Chi-squared tests or Fisher's exact test, as appropriate.

For clinical studies, the baseline characteristics and levels of IL-16 between normal patients and patients with sarcopenia were compared and then propensity score matching (PSM) was performed to reduce the bias caused by the co-factors. Spearman's rank correlation coefficient was employed to assess the degree of association between serum IL-16 and sarcopenia traits. The receiver operating characteristic (ROC) curves were established to evaluate the roles of IL-16 in sarcopenia and to identify the most suitable cutoff values of IL-16 based on the Youden index. Then the populations were divided into two groups (with normal IL-16 and high IL-16) according to the cutoff values of IL-16. The sarcopenia traits were compared between the populations grouped by IL-16. Furthermore, logistics models were established to further identify the relationships between IL-16 and sarcopenia by reducing the impact caused by co-variables.

A P value < 0.05 was considered to be significant. All statistical analyses were performed by using R software version 4.2.2 (R Foundation for Statistical Computing, Vienna, Austria) and GraphPad Prism version 8.0.1 (GraphPad Software, San Diego, CA).

Results

General features of participants and PSM

Finally, a total of 421 individuals were included in the clinical study. The detailed numbers of exclusion are summarized in Fig. 1. In all individuals, the mean age is 75.80 ± 8.55 years old, and 288 (68.41%) of them were females. In all populations, 77 individuals were identified as sarcopenia, and the mean age of them was 79.13 ± 9.25 years old, while the mean age of those without sarcopenia was 75.05 ± 8.21 years old. The populations with sarcopenia were significantly older than normal adults ($p < 0.001$). Except the age, there were no significant differences in other baseline variables (all $p > 0.05$). The baseline characteristics are summarized in Table 1. Therefore, we conducted the PSM with a caliper of 0.2 to reduce the potential bias caused by different ages between groups. After PSM, the dataset was reduced from 421 individuals to 144 (72 sarcopenia cases and 72 matched controls), representing a 65.8% loss of cases. Specifically, the normal group decreased from 344 to 72 individuals, a reduction of 79.1%. This substantial loss of cases is attributed to the strict matching criteria necessary to ensure covariate balance and minimize bias. Despite the reduced sample size, the matched groups exhibited no significant differences in baseline characteristics, ensuring comparability

Table 1 Baseline characteristics of unmatched populations

Variables	All individuals (*n* = 421)	Normal (*n* = 344)	Sarcopenia (*n* = 77)	*p* value Normal vs. Sarcopenia
Sex(female)	288 (68.41%)	234 (68.02%)	54 (70.13%)	0.823
Age(years)	75.80 ± 8.55	75.05 ± 8.21	79.13 ± 9.25	< 0.001
BMI (kg/m^2)	21.72 ± 4.33	21.62 ± 4.28	22.20 ± 4.58	0.276
Fractures history (yes)	71 (16.86%)	59 (17.15%)	12 (15.58%)	0.87
Smoking history (yes)	46 (10.93%)	41 (11.92%)	5 (6.49%)	0.239
Alcoholism history(yes)	21 (4.99%)	17 (4.94%)	4 (5.19%)	> 0.999
CCI score (> 4)	119 (28.27%)	95 (27.62%)	24 (31.17%)	0.627
Electrocardiogram (abnormal)	248 (58.91%)	196 (56.98%)	52 (67.53%)	0.116
Chest radiograph (abnormal)	224 (53.21%)	178 (51.74%)	46 (59.74%)	0.252
Hypertension(yes)	223 (52.97%)	185 (53.78%)	38 (49.35%)	0.564
RBC (10^12/L)	4.54 ± 0.60	4.52 ± 0.58	4.62 ± 0.65	0.438
Hb (g/L)	94.58 ± 13.82	94.29 ± 13.66	95.86 ± 14.57	0.288
ALB (g/L)	38.63 ± 9.05	38.51 ± 8.97	39.17 ± 9.44	0.624
GLU (mmol/L)	6.18 ± 1.49	6.17 ± 1.50	6.25 ± 1.48	0.839

Note: P-values indicate comparisons between the Normal and Sarcopenia groups. Continuous variables were expressed as mean ± standard deviation and categorical variables were presented as count (percent). BMI, body mass index; Hb, Hemoglobin; RBC, red blood count; GLU, blood glucose; ALB, albumin

between the sarcopenia and non-sarcopenia groups. (Table 2).

Relationships between IL-16 and sarcopenia

In the raw populations, the serum levels of IL-16 were significantly correlated with HGS negatively (Spearman r: -0.107, $p = 0.028$, Fig. 2A) while not significantly with ASM (Spearman r: -0.045, $p = 0.357$, Fig. 2B). Then, we compared the serum levels of IL-16 between patients with different sarcopenia status. The individuals with low HGS ($p < 0.001$, Fig. 2C) or with sarcopenia ($p < 0.001$, Fig. 2E) may have high levels of IL-16. The levels of IL-16 between individuals with normal or low ASM were not significantly different ($p = 0.093$, Fig. 2D). Similarly in ROC curves, the area under the receiver operating characteristic (AUROC) of IL-16 for low HGS, low ASM, and sarcopenia were 0.610, 0.549, and 0.662 (Fig. 2F and H).

In the matched populations, the correlation between IL-16 and HGS, as well as ASM was both significant (for HGS: Spearman r: -0.271, $p = 0.001$; Spearman r: -0.265, $p = 0.001$, Fig. 2I and J). The serum levels of IL-16 of individuals with low HGS, ASM, and sarcopenia were significantly higher than normal individuals (all $p < 0.001$, Fig. 2K and M). In the ROC curves, the AUROC of IL-16 for low HGS, low ASM, and sarcopenia were 0.709, 0.697, and 0.701 (Fig. 2N and P).

Based on the Youden index based on ROC curves of IL-16 for sarcopenia in the matched populations, the 10.90 pg/mL was calculated as the cutoff value of IL-16: the individuals with IL-16 > 10.90 pg/mL were identified as high levels of IL-16. In all populations, 34 of them were identified with high levels of IL-16. Then, we compared the sarcopenia traits of participants with different IL-16 levels. The adults with high levels of IL-16 may have significantly low HSG and ASM and may have high proportions of low HSG, low ASM, and sarcopenia (all $p < 0.001$, Table 3).

Lastly, the univariate and multivariate logistics models were established to reduce the potential bias caused by co-variables. The multivariate models 1 were adjusted for age, and the multivariate models 2 were adjusted for the variables selected by stepwise methods (age and electrocardiogram). As shown in Table 4, all models prove that individuals with high levels of IL-16 may have a significantly higher risk of sarcopenia (all $p < 0.001$, Table 4).

IL-16 impairs muscle function and physical performance

Based on the results from the population study, we further conducted animal research to identify the roles of IL-16 in sarcopenia. Starting from the age of 14 months, mice were administered IL-16 via systemic injection until they reached 20 months of age. To assess the efficacy of IL-16 administration, we measured the serum levels of IL-16 in mice at the ages of 17 and 20 months. As shown in Fig. 3A, the serum IL-16 levels in the IL-16 treated group (17 months: 220.10 ± 23.94 pg/mL; 20 months: 214.1 ± 47.59 pg/mL) were significantly higher compared to the control group (17 months: 103.3 ± 24.17 pg/mL; 20 months: 102.5 ± 24.34 pg/mL), indicating a successful delivery and systemic presence of IL-16. During this period, we continuously monitored the body weight of the mice, measuring it once a month as depicted in Fig. 3B. The control group mice exhibited a steady increase in body weight, while the IL-16 treated group showed a sustained decrease in body weight. The body weight of the treated group was significantly lower than that of the control group from month 17 onward.

At the ages of 17 and 20 months, we conducted muscle function tests and assessments of locomotor ability in the mice. Specifically, at 17 months of age, the IL-16 treated

Table 2 Baseline characteristics of matched populations

Variables	All individuals ($n = 144$)	Normal ($n = 72$)	Sarcopenia ($n = 72$)	*p* value Normal vs. Sarcopenia
Sex(female)	103 (71.53%)	51 (70.83%)	52 (72.22%)	> 0.999
Age(years)	78.02 ± 8.17	77.88 ± 7.62	78.17 ± 8.75	0.793
BMI (kg/m^2)	22.33 ± 4.34	22.64 ± 4.12	22.03 ± 4.56	0.477
Fractures history (yes)	24 (16.67%)	13 (18.06%)	11 (15.28%)	0.823
Smoking history (yes)	7 (4.86%)	2 (2.78%)	5 (6.94%)	0.438
Alcoholism history(yes)	10 (6.94%)	6 (8.33%)	4 (5.56%)	0.743
CCI score (> 4)	43 (29.86%)	22 (30.56%)	21 (29.17%)	> 0.999
Electrocardiogram (abnormal)	98 (68.06%)	51 (70.83%)	47 (65.28%)	0.592
Chest radiograph (abnormal)	83 (57.64%)	42 (58.33%)	41 (56.94%)	> 0.999
Hypertension(yes)	76 (52.78%)	38 (52.78%)	38 (52.78%)	> 0.999
RBC (10^12/L)	4.55 ± 0.64	4.48 ± 0.62	4.62 ± 0.66	0.393
Hb (g/L)	95.19 ± 14.13	95.05 ± 13.64	95.33 ± 14.71	0.868
ALB (g/L)	38.92 ± 9.19	38.67 ± 9.04	39.17 ± 9.40	0.739
GLU (mmol/L)	6.28 ± 1.50	6.32 ± 1.49	6.25 ± 1.51	0.603

Note: P-values indicate comparisons between the Normal and Sarcopenia groups. Continuous variables were expressed as mean ± standard deviation and categorical variables were presented as count (percent). BMI, body mass index; Hb, Hemoglobin; RBC, red blood count; GLU, blood glucose; ALB, albumin

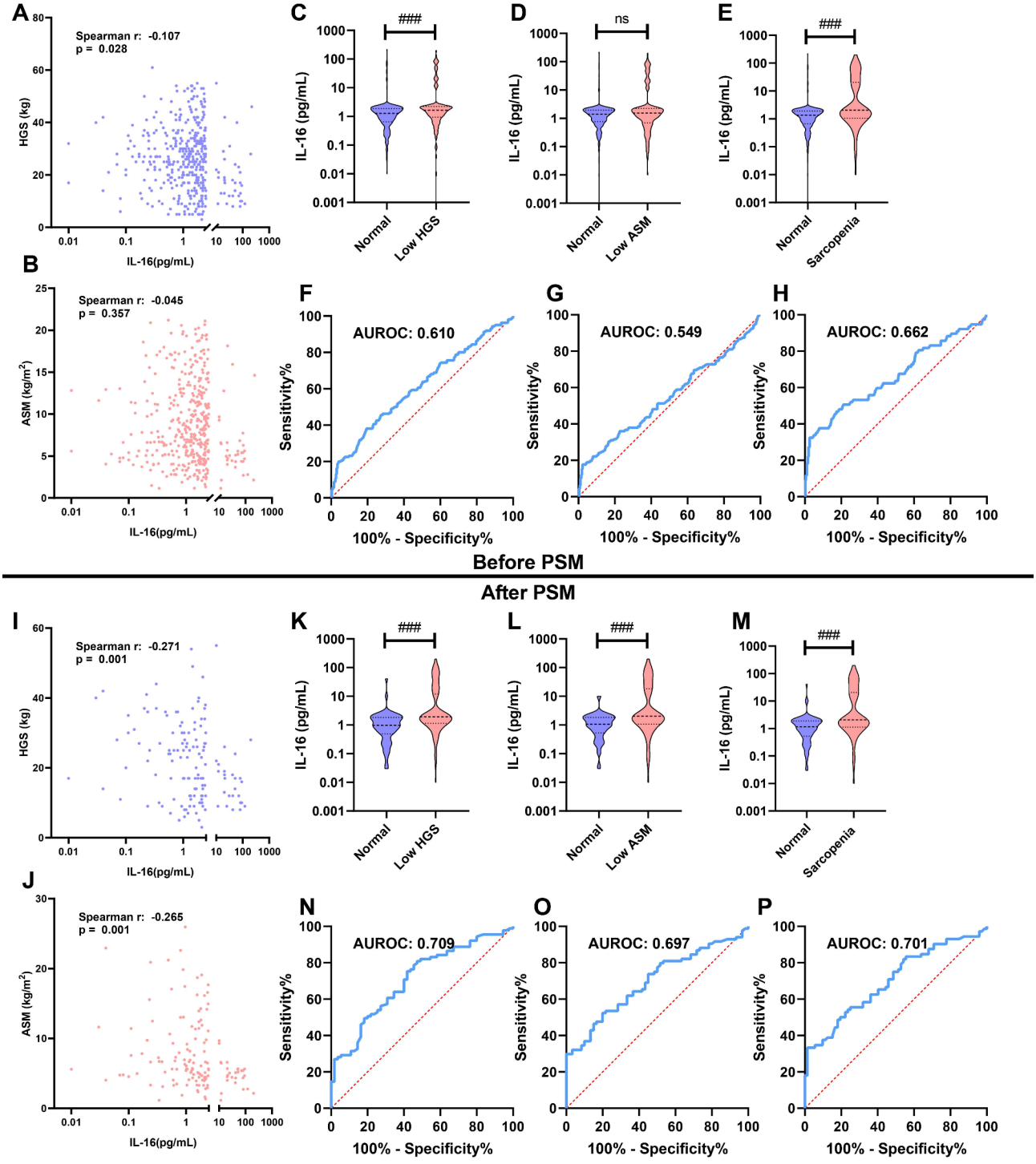

Fig. 2 Relationships between IL-16 and sarcopenia. **A**: correlations between IL-16 and HGS based on raw populations; **B**: correlations between IL-16 and ASM based on raw populations; **C**: comparison of IL-16 between normal groups and low HGS groups based on raw populations; **D**: comparison of IL-16 between normal groups and low ASM groups based on raw populations; **E**: comparison of IL-16 between normal groups and sarcopenia groups based on raw populations; **F**: ROC curves of IL-16 for low HGS based on raw populations; **G**: ROC curves of IL-16 for low ASM based on raw populations; **H**: ROC curves of IL-16 for sarcopenia based on raw populations; **I**: correlations between IL-16 and HGS based on matched populations; **J**: correlations between IL-16 and ASM based on matched populations; **K**: comparison of IL-16 between normal groups and low HGS groups based on matched populations; **L**: comparison of IL-16 between normal groups and low ASM groups based on matched populations; **M**: comparison of IL-16 between normal groups and sarcopenia groups based on matched populations; **N**: ROC curves of IL-16 for low HGS based on matched populations; **O**: ROC curves of IL-16 for low ASM based on matched populations; **P**: ROC curves of IL-16 for sarcopenia based on matched populations

Table 3 Sarcopenia traits of individuals grouped by IL-16 levels

Variables	Normal levels IL-16 (*n* = 387)	High levels of IL-16 (*n* = 34)	Effect size	*p* value
HSG (kg)	26.49 ± 12.09	18.62 ± 9.88	Cohen's d = 0.660	< 0.001
ASM (kg/m2)	9.39 ± 5.22	6.05 ± 3.80	Cohen's d = 0.652	< 0.001
Low HSG (yes)	134 (34.63%)	26 (76.47%)	Odd ratio = 6.136	< 0.001
Low ASM (yes)	130 (33.59%)	28 (82.35%)	Odd ratio = 9.226	< 0.001
Sarcopenia (yes)	52 (13.44%)	25 (73.53%)	Odd ratio = 17.895	< 0.001

Note: Continuous variables were expressed as mean ± standard deviation and categorical variables were presented as count (percent). Effect sizes for continuous variables are reported as Cohen's d, and for categorical variables as odds ratios. HGS: hand grip strength; ASM: appendicular skeletal muscle mass

Table 4 Results of logistics analysis

Variables	Univariate models		Multivariate models 1		Multivariate models 2	
	OR (95% CI)	*p*	OR (95% CI)	*p*	OR (95% CI)	*p*
IL-16 (continuous)	1.036 [1.021, 1.054]	< 0.001	1.034 [1.019, 1.052]	< 0.001	1.034 [1.019, 1.053]	< 0.001
IL-16 (> 10.90 pg/mL)	17.895 [8.181, 42.556]	< 0.001	19.527 [8.675, 47.886]	< 0.001	19.846 [8.790, 48.782]	< 0.001

Note: OR: odd ratio; CI: confidence interval. Multivariate models 1 were adjusted for age; Multivariate models 2 were adjusted for age and electrocardiogram (variables selected by stepwise selection methods)

mice demonstrated a significant reduction in exhaustion distance compared to the control group during exercise. At 20 months of age, the IL-16 treated mice showed a significant decrease in both the distance and time to exhaustion compared to the control group (Fig. 3C). The insignificant reduction in exhaustion time at 17 months may be caused by the distribution of distance change. In our study, exhaustion was determined when a mouse's hindlimbs remained in contact with the electric grid for over 15 s. The different contact times may cause uncorrelated results.

To ascertain the post-exhaustion muscle repair capacity in mice, dropout experiments were initiated after the mice had a full 24-hour rest period. Each instance where a mouse made contact with the electric grid was recorded as a dropout. The control group mice exhibited minimal dropouts only at speeds reaching 12 m/s, with data at 17 months and 20 months of age being largely consistent. In contrast, the IL-16 treated mice began to dropout at 10 m/s, and the number of dropouts increased with higher speeds. At 20 months of age, the number of dropouts in the IL-16 group was higher compared to the 17-month age mark (Fig. 3D).

IL-16 leads to muscle atrophy

Next, we explored the roles of IL-16 in muscle mass and muscle atrophy [14]. At 20 months of age, the IL-16 treated mice showed a significantly low mass of quadriceps (QU) and gastrocnemius (GA) compared with the control group, while at 17 months of age, only GA was significantly decreased (Supplementary Fig. 1A). To reduce the bias caused by whole body mass, we further adjusted the mass of QU and GA for body mass. After adjustment, at both the ages of 17 and 20 months, the proportions of mass of QU and GA in the IL-16 treated group were significantly lower than the control group (Fig. 3E). Significant increases in the total lipid percentage of the treated group were observed at both 17 and 20 months, indicating that IL-16 also promotes intermuscular lipid deposition (Fig. 3F). We also investigated the effects of IL-16 administration on related inflammatory factors. It was found that while IL-16 treatment induced a modest increase in serum IL-6 and TNFα levels, these increases were not statistically significant (Supplementary Fig. 1B). In the H&E staining and immunofluorescence staining of muscles, the fiber sizes of IL-16 treated mice were smaller than normal mice (Fig. 3G). The quantification analysis showed that the IL-16 treated groups may have significantly lower mean CSA compared to control groups. Similarly, we examined the gene expression levels of myosin heavy chain (MHC) subtypes and found that IL-16 administration significantly reduced the gene expression of MHC-IIb, while no significant effects were observed on the other subtypes, including MHC-I, MHC-IIa, and MHC-IIx (Fig. 3H).

Anti-IL-16 inhibits the development of muscle atrophy caused by BoNT/A

We next established the sarcopenia models using BoNT/A and all the tests were conducted at 20 months of age. Mice were administered an intramuscular injection of 1 unit (U) of BoNT/A, evenly distributed into both limbs, with a total injection volume of 20 μL of physiological saline, administered biweekly. In the meantime, the BoNT/A mice were treated with mouse IgG or anti-IL-16 antibody to identify the potential therapeutical effect of anti-IL-16. The measurements of serum IL-16 levels are depicted in Fig. 4A. Interestingly, while we observed a trend towards increased IL-16 levels in the BoNT/A + IgG treated group, this elevation did not reach statistical significance ($p > 0.05$) compared to the control group. Previous studies have indicated that botulinum

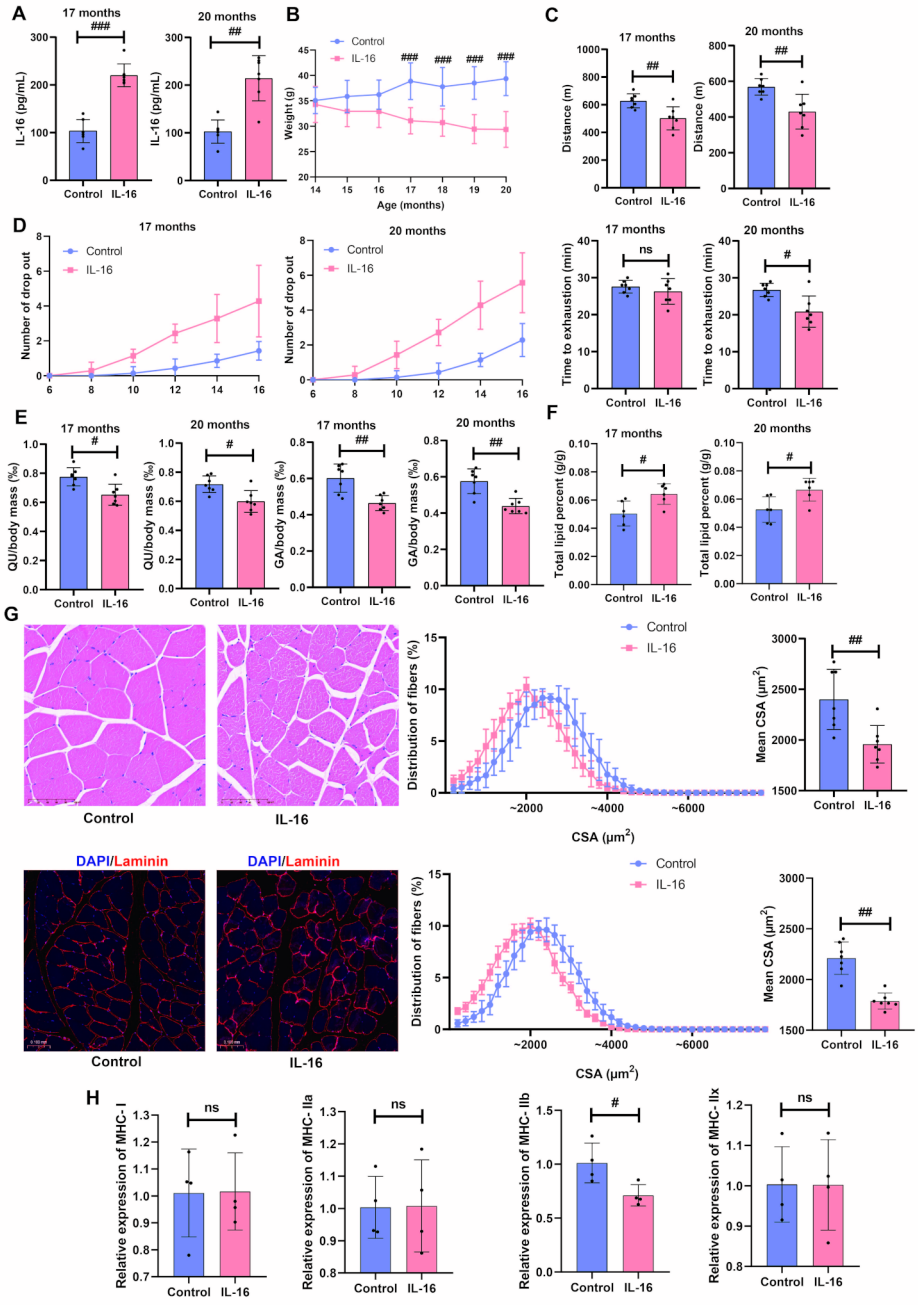

Fig. 3 IL-16 impairs muscle function and physical performance and leads to muscle atrophy in mice. **A**: measurement of serum IL-16 levels of mice with ($n=7$) or without ($n=7$) IL-16 treatment; **B**: changes of weight of mice with ($n=14$) or without ($n=14$) IL-16 treatment; **C**: comparison of distance and time to exhaustion between mice with ($n=7$) or without ($n=7$) IL-16 treatment; **D**: comparison of numbers of drop out between mice with or ($n=7$) without ($n=7$) IL-16 treatment; **E**: comparison of QU/body mass and GA/body mass between mice with ($n=7$) or without ($n=7$) IL-16 treatment; **F**: comparison of total lipid percentage of QU from mice with ($n=6$) or without ($n=6$) IL-16 treatment; G:H&E staining, immunofluorescence staining, and quantification of fiber distribution and mean CSA of mice with ($n=7$) or without ($n=7$) IL-16 treatment; H: qRT-PCR results of mice with ($n=4$) or without ($n=4$) IL-16 treatment

toxin may lead to increased transcription of IL-6 and TNFα [15]. The cascade effect of these pro-inflammatory cytokines may contribute to the elevation of IL-16 levels. Compared with the control group and BoNT/A + IgG treated group, the BoNT/A + anti-IL-16 mice showed significantly lower IL-16 levels, which indicated the effectiveness of targeting IL-16. Moreover, the anti-IL-16 treatment resulted in a significant decrease in IL-16 levels below those of the control group, which suggested that the primary effect of our treatment is to reduce

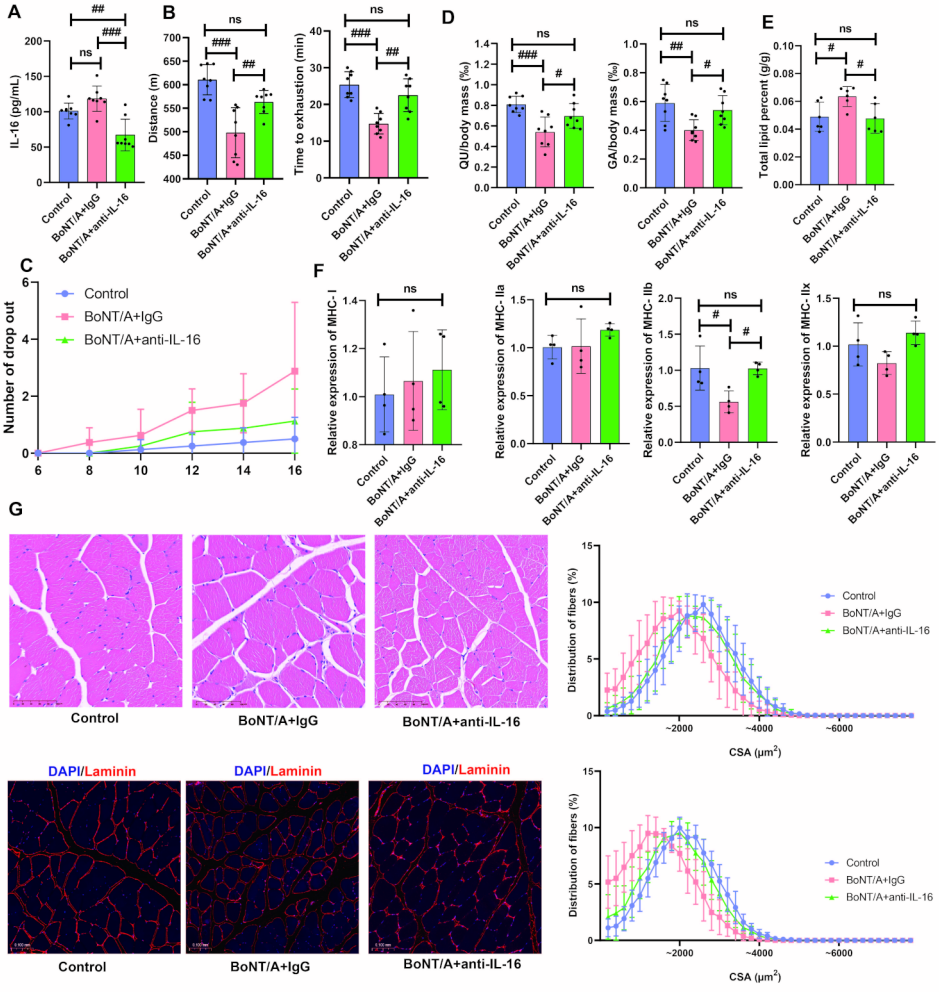

Fig. 4 Anti-IL-16 inhibits the development of muscle atrophy caused by BoNT/A. **A**: measurement of serum IL-16 levels of the control group ($n=8$), BoNT/A + IgG group ($n=8$), and BoNT/A + anti-IL-16 group ($n=8$); **B**: comparison of distance and time to exhaustion between the control group ($n=8$), BoNT/A + IgG group ($n=8$), and BoNT/A + anti-IL-16 group ($n=8$); **C**: comparison of numbers of drop out between control group ($n=8$), BoNT/A + IgG group ($n=8$), and BoNT/A + anti-IL-16 group ($n=8$); **D**: comparison of QU/body mass and GA/body between the control group ($n=8$), BoNT/A + IgG group ($n=8$), and BoNT/A + anti-IL-16 group ($n=8$); **E**: comparison of total lipid percentage of QU from mice the control group ($n=6$), BoNT/A + IgG group ($n=6$), and BoNT/A + anti-IL-16 group ($n=6$); **F**: qRT-PCR results of the control group ($n=4$), BoNT/A + IgG group ($n=4$), and BoNT/A + anti-IL-16 group ($n=4$); G: H&E staining, immunofluorescence staining, and quantification of fiber distribution of the control group ($n=8$), BoNT/A + IgG group ($n=8$), and BoNT/A + anti-IL-16 group ($n=8$)

IL-16 levels below the baseline, rather than simply counteracting an increase. The BoNT/A + IgG mice showed significantly impaired muscle functions and low muscle mass compared with control mice. The BoNT/A + IgG mice showed a significant decrease in both the distance and time to exhaustion and these effects could be reduced by using anti-IL-16 antibody (Fig. 4B). Similarly in the dropout tests, the BoNT/A + anti-IL-16 mice showed fewer numbers of dropout than BoNT/A + IgG mice (Fig. 4C). However, the effects of anti-IL-16 on the absolute QU and GA mass were not significant (Supplementary Fig. 1C), while after adjusting for whole body mass, the effects showed significance (Fig. 4D). Compared to the control group, BoNT/A + IgG mice exhibited increased total muscle lipid deposition, an effect attenuated by anti-IL-16 treatment (Fig. 4E). In terms of inflammatory cytokines, BoNT/A + IgG elevated IL-6 and TNFα levels; however, while anti-IL-16 slightly reduced these effects, the differences were non-significant (Supplementary Fig. 1D). Similarly, in MHC expression, only MHC-IIb showed a statistically significant difference (Fig. 4F). Lastly, based on H&E and Laminin staining, the BoNT/A + IgG mice may have significantly lower mean CSA compared with BoNT/A + anti-IL-16 mice (Fig. 4G and Supplementary Fig. 1E).

Discussion

In this study, by integrating the evidence from patients and animals, we comprehensively explored the roles of IL-16 in the development of sarcopenia. In the clinical study, we enrolled the geriatric orthopedic patients in our department to primarily identify the relationships between serum IL-16 and sarcopenia: the patients with high levels of serum IL-16 may have a significantly higher risk of sarcopenia. In the relationships between IL-16 and the meta-traits of sarcopenia, the results also indicated that high levels of IL-16 may relate to low HGS and ASM. To address the potential impact caused by co-variables, such as age and sex, we conducted PSM and established multivariate logistics models, and all results suggested the roles of IL-16 in sarcopenia.

The roles of IL-16 in sarcopenia have been reported in recent studies. In an observational study including 225 patients with gastric cancer, the individuals with sarcopenia had significantly high IL-16 expression, and both sarcopenia and IL-16 were identified as independent risk factors for overall survival and relapse-free survival [16]. A study conducted in Germany with 80 older participants also reported a similar conclusion: high levels of serum IL-16 were proven to be the risk factor for sarcopenia in females while being the protective factor in males [17]. However, in our study, there are no significant differences in the factor of sex (Tables 1 and 2). We believe this may be attributed to our larger sample size. In the subgroup analysis based on our cohorts, the patients with sarcopenia may have significantly high levels of serum IL-16 in both males (4.00 ± 21.18 pg/mL vs. 26.07 ± 48.37 pg/mL, $p = 0.006$) and females (2.41 ± 8.42 pg/mL vs. 15.19 ± 27.60 pg/mL, $p < 0.001$).

However, the mentioned clinical studies may be limited to a small sample size and lack evidence of causality. Some researchers tried to estimate the causal roles of IL-16 in sarcopenia by using Mendelian randomization methods and the roles of IL-16 in sarcopenia were still controversial: the high levels of IL-16 were estimated to low risk of low HGS but to high risk of low ASM [10]. Therefore, we continually conducted animal studies to further complement the evidence of the roles of IL-16 in sarcopenia.

Compared to the control group, the mice treated with IL-16 showed a decrease in body weight, muscle function, and muscle mass. The functional decline in muscle performance, as evidenced by the dropout experiment, is a critical finding of our study. The IL-16 treated mice exhibited an earlier onset of exhaustion and a reduced capacity to tolerate high-intensity exercise, indicating compromised muscle endurance. For the muscle mass, the sustained muscle loss in the IL-16 group suggests a potential role for IL-16 in the regulation of body composition, particularly in the context of muscle protein balance. Furthermore, the sarcopenia models were established and treated by anti-IL-16 antibodies, which may potentially suggest the therapeutical effect of targeting IL-16. We also observed similar phenotypes in MHC-IIb expression and intramuscular total lipid deposition. Inflammatory cytokine levels showed that anti-IL-16 slightly reduced IL-6 and TNFα levels, but this effect was not significant and requires further research. The results indicated that anti-IL-16 may significantly rescue impaired muscle function and muscle atrophy in mice, despite the non-significant effects on inflammatory cytokines.

The potential mechanism of IL-16 in the development of sarcopenia can be discussed from an immunological perspective, considering its role as a cytokine involved in inflammatory responses [18]. IL-16 is known to modulate T-cell activation and chemotaxis, which may influence muscle homeostasis [19]. In the context of sarcopenia, chronic low-grade inflammation, or "inflammaging," is characterized by an increase in pro-inflammatory cytokines such as IL-6 and TNF-α, which can lead to muscle wasting [20]. It is plausible that IL-16, through its effects on immune cell function, may contribute to this inflammatory milieu, potentially exacerbating muscle atrophy [21]. Furthermore, IL-16 expression has been associated with the activation of catabolic pathways in muscle cells by influencing the NF-κB signaling pathway, which is known to regulate the expression of atrophy-related genes such as MuRF-1 and MAFbx [22, 23]. These genes are involved in the ubiquitin-proteasome pathway, leading to muscle protein degradation and contributing to sarcopenia [24]. Therefore, IL-16 could be a link between immune system activation and muscle wasting, highlighting its potential as a therapeutic target for interventions aimed at preventing or treating sarcopenia.

Though few studies reported the mechanism of IL-16 in skeletal muscles, many understandings of IL-16 in vascular smooth muscle and heart muscle. The mice with enhanced expression of IL-16 may have cardiac fibrosis and LV myocardial stiffening accompanied by increased macrophage infiltration [25]. The mice treated with IL-16 may also have increased vascular smooth muscle cell migration and invasion and increased MMP-9 expression in vascular smooth muscle cells, which was induced by IL-16 via regulating the activity of NF-κB, AP-1, and Sp-1 motifs [26]. IL-16 may also contribute to cardiac injury via the Nrf2 pathway [27].

This study is subject to several limitations that must be recognized. First, this study included the patients in the department of orthopedics and all the individuals may face the impact of fracture or trauma, which may compromise the results of our findings. However, we set strict inclusion and exclusion criteria and controlled the differences in the baseline features by PSM, which may

thoroughly reduce the bias caused by co-factors. Secondly, the assessment of sarcopenia was conducted upon the patients' initial hospital admission, often under limited physical conditions due to their fractures. Despite this, a uniform measurement protocol was applied to all participants, which helped to reduce any bias that could be attributed to the patients' postures. Thirdly, the clinical study's observational nature limits our ability to infer causality between sarcopenia indicators and outcomes related to fractures, but in the animal study, we further proved that IL-16 may contribute to the development of sarcopenia. Fourthly, the use of 1:1 propensity score matching (PSM) resulted in a reduction of the sample size. Although we attempted higher matching ratios, these approaches led to incomplete matching for several key covariates. Therefore, we opted for 1:1 PSM to ensure covariate balance. Moreover, it is important to note that the sample sizes in our study were constrained by the high mortality rate observed in aged mice, which may impact the statistical power of our findings. Another limitation of animal study was the absence of grip strength measurements. While our assessments of time to exhaustion, distance traveled, and dropout counts were well-established metrics of muscle endurance and fatigue, grip strength testing is recognized as a valuable complementary measure. Lastly, we did not further explore the mechanism of IL-16 in sarcopenia in animal research. Future studies should aim to elucidate the intracellular signaling cascades activated by IL-16 in skeletal muscle to better understand its role in muscle atrophy.

In conclusion, our integrated study provides novel insights into the role of IL-16 in age-related skeletal muscle atrophy. The findings suggest that IL-16 may be a key player in the muscle-wasting process, with potential therapeutic implications for mitigating sarcopenia.

Supplementary Information

The online version contains supplementary material available at https://doi.org/10.1186/s12891-025-08633-9.

Supplementary Material 1

Acknowledgements
Not applicable.

Author contributions
All authors (Fan Wenliang, Zhao Zhibang, Wang Liqiang, and Chu Qingbo) made a significant contribution to the work reported, whether that is in the conception, study design, execution, acquisition of data, analysis, and interpretation, or in all these areas; took part in drafting, revising, or critically reviewing the article; gave final approval of the version to be published; have agreed on the journal to which the article has been submitted; and agree to be accountable for all aspects of the work.

Funding
Not applicable.

Data availability
The datasets used and/or analyzed during the current study are available from the corresponding author upon reasonable request.

Declarations

Ethics approval and consent to participate
We declare that this study was conducted in accordance with the Declaration of Helsinki, and approved by the Ethics Committee of Nanyang Second People's Hospital (ID: 2020 Research Review No. 11) and the Animal Ethics Committee of Nanyang Second People's Hospital (ID: 2021 Animal Research Review No. 2). All the information about patient privacy was well protected, and written informed consent was obtained from all patients enrolled in this study.

Conflict of interest
The authors declare that they have no conflict of interest.

Clinical trial number
Not applicable.

Received: 8 February 2025 / Accepted: 8 April 2025
Published online: 17 April 2025

References

1. Chen LK, Woo J, Assantachai P, Auyeung TW, Chou MY, Iijima K, Jang HC, Kang L, Kim M, Kim S, Kojima T, Kuzuya M, Lee JSW, Lee SY, Lee WJ, Lee Y, Liang CK, Lim JY, Lim WS, Peng LN, Sugimoto K, Tanaka T, Won CW, Yamada M, Zhang T, Akishita M. and H. Arai, Asian Working Group for Sarcopenia: 2019 Consensus Update on Sarcopenia Diagnosis and Treatment. J Am Med Dir Assoc 21 (2020) 300–307 e2.
2. Stefanakis K, Kokkorakis M, Mantzoros CS. The impact of weight loss on fat-free mass, muscle, bone and hematopoiesis health: Implications for emerging pharmacotherapies aiming at fat reduction and lean mass preservation. Metabolism (2024) 156057.
3. Qu Y, Zhang L, Liu Y, Fu Y, Wang M, Liu C, Wang X, Wan Y, Xu B, Zhang Q, Li Y, Jiang P. Development and validation of a predictive model assessing the risk of sarcopenia in rheumatoid arthritis patients. Front Immunol. 2024;15:1437980.
4. Liu M, Yu D, Pan Y, Ji S, Han N, Yang C, Sun G. Causal roles of lifestyle, psychosocial characteristics, and sleep status in sarcopenia: A Mendelian randomization study. J Gerontol Biol Sci Med Sci 79 (2024).
5. O'Rourke SA, Shanley LC, Dunne A. The Nrf2-HO-1 system and inflammaging. Front Immunol. 2024;15:1457010.
6. Muller L, Di Benedetto S. From aging to long COVID: exploring the convergence of Immunosenescence, inflammaging, and autoimmunity. Front Immunol. 2023;14:1298004.
7. Liu M, Wang J, Han Y, Fu X, Pan Y, Yang C, Sun G. Comprehensive landscapes of the causal network between immunity and sarcopenia. Front Immunol. 2024;15:1443885.
8. Ravalet N, Guermouche H, Hirsch P, Picou F, Foucault A, Gallay N, Martignoles JA, Beaud J, Suner L, Deswarte C, Lachot S, Rault E, Largeaud L, Gissot V, Bene MC, Gyan E, Delhommeau F, Herault O. Modulation of bone marrow and peripheral blood cytokine levels by age and clonal hematopoiesis in healthy individuals. Clin Immunol. 2023;255:109730.
9. Kornfeld H, Cruikshank WW. Prospects for IL-16 in the treatment of AIDS. Expert Opin Biol Ther. 2001;1:425–32.
10. Liu M, Fu X, Yu D, Li M, Pan Y, Yang C, Sun G. Mapping the causal associations of cytokines with sarcopenia and aging traits: evidence from bidirectional Mendelian randomization. J Cachexia Sarcopenia Muscle. 2024;15:1121–33.
11. Ma S, Xing X, Huang H, Gao X, Xu X, Yang J, Liao C, Zhang X, Liu J, Tian W, Liao L. Skeletal muscle-derived extracellular vesicles transport glycolytic enzymes to mediate muscle-to-bone crosstalk. Cell Metab. 2023;35:2028–43. e7.
12. Yang SJ, Chang ST, Chang KC, Lin BW, Chang KY, Liu YW, Lai MD, Hung LY. Neutralizing IL-16 enhances the efficacy of targeting Aurora-A therapy in colorectal cancer with high lymphocyte infiltration through restoring antitumor immunity. Cell Death Dis. 2024;15:103.

13. Park K, Jung S, Ha JH, Jeong Y. Protaetia brevitarsis hydrolysate mitigates muscle dysfunction and ectopic fat deposition triggered by a High-Fat diet in mice. Nutrients 17 (2025).
14. Li H, Wang P, Zhang C, Zuo Y, Zhou Y, Han R. Defective BVES-mediated feedback control of cAMP in muscular dystrophy. Nat Commun. 2023;14:1785.
15. Pingel J, Nielsen MS, Lauridsen T, Rix K, Bech M, Alkjaer T, Andersen IT, Nielsen JB, Feidenhansl R. Injection of high dose botulinum-toxin A leads to impaired skeletal muscle function and damage of the fibrilar and non-fibrilar structures. Sci Rep. 2017;7:14746.
16. Xiong J, Hu H, Kang W, Shao X, Li Y, Jin P, Tian Y. Association of sarcopenia and expression of Interleukin-16 in gastric cancer survival. Nutrients 14 (2022).
17. Chen Z, Laurentius T, Fait Y, Muller A, Muckter E, Hao D, Bollheimer LC, Nourbakhsh M. Sex-Specific associations between serum IL-16 levels and sarcopenia in older adults. Nutrients 15 (2023).
18. Maione F, Iqbal AJ, Raucci F, Letek M, Bauer M, D'Acquisto F. Repetitive exposure of IL-17 into the murine air pouch favors the recruitment of inflammatory monocytes and the release of IL-16 and TREM-1 in the inflammatory fluids. Front Immunol. 2018;9:2752.
19. Gonzalez-Rodriguez S, Sordo-Bahamonde C, Alvarez-Artime A, Baamonde A, Menendez L. Hyperalgesic effect evoked by il-16 and its participation in inflammatory hypernociception in mice. J Neuroimmune Pharmacol. 2024;19:44.
20. Jurcau MC, Jurcau A, Cristian A, Hogea VO, Diaconu RG, Nunkoo VS. Inflammaging and brain aging. Int J Mol Sci 25 (2024).
21. Xiao J, Li HS, Satyanarayanan SK, Leung SL, Yuan Q, Wang Y, Qin D. and S.M. Yan Lee, Advancements in Targeting Macrophage Senescence for Age-Associated Conditions. Aging Dis (2024).
22. Zhou Z, Zhang P. Formononetin ameliorates the LPS-induced inflammatory response and apoptosis of neuronal cells via NF-kappaB/NLRP3 signaling pathway. Funct Integr Genomics. 2023;23:321.
23. Zhang H, Du Y, Tang W, Chen M, Yu W, Ke Z, Dong S, Cheng Q. Eldecalcitol prevents muscle loss and osteoporosis in disuse muscle atrophy via NF-kappaB signaling in mice. Skelet Muscle. 2023;13:22.
24. Oh S, Yang JY, Park CH, Son KH, Byun K. Dieckol reduces muscle atrophy by modulating angiotensin type II type 1 receptor and NADPH oxidase in spontaneously hypertensive rats. Antioxid (Basel) 10 (2021).
25. Tamaki S, Mano T, Sakata Y, Ohtani T, Takeda Y, Kamimura D, Omori Y, Tsukamoto Y, Ikeya Y, Kawai M, Kumanogoh A, Hagihara K, Ishii R, Higashimori M, Kaneko M, Hasuwa H, Miwa T, Yamamoto K, Komuro I. Interleukin-16 promotes cardiac fibrosis and myocardial stiffening in heart failure with preserved ejection fraction. PLoS ONE. 2013;8:e68893.
26. Park SL, Hwang B, Lee SY, Kim WT, Choi YH, Chang YC, Kim WJ, Moon SK. p21WAF1 is required for Interleukin-16-Induced migration and invasion of vascular smooth muscle cells via the p38MAPK/Sp-1/MMP-9 pathway. PLoS ONE. 2015;10:e0142153.
27. Zhang J, Yang Z, Liang Z, Wang M, Hu C, Chang C, Shi L, Ji Q, Liu L. Anti-Interleukin-16 Neutralizing Antibody Treatment Alleviates Sepsis-Induced Cardiac Injury and Dysfunction via the Nuclear Factor Erythroid-2 Related Factor 2 Pathway in Mice. Oxid Med Cell Longev 2021 (2021) 6616422.

Publisher's note